CONF-781202--33

"On the Use of the Finite Element Displacement Method to Solve Solid-Fluid Interaction Vibration Problems"

By

S. J. Brown
K. H. Hsu

Babcock & Wilcox Co., Nuclear Equipment Division

950 5366

1.0 INTRODUCTION

The study of the influence of fluids interacting with structural vibration and dynamic behavior has been of interest for hundreds of years. In 1779 Pierre Louis Gabriel Du Buat published the results of pendulum bobs vibration in air and water that showed an apparent change in mass through a water influenced reduction of the frequency. Since that time, many solid-fluid interaction problems have been investigated by many methods. Because of the complexity of the solution of the general field equations in a Eulerian frame, the analyst has been required to consider special cases or instances where variable or boundary simplification results in a more tractable problem. Generally fluid-structural interaction problems may be divided into strong and weak coupling problems such as discussed in symposium volumes (1, 2, 3). With the lack of coupling we have structural problems treated usually in a Lagrangian sense and fluid problems dealt with in a Eulerian frame. Even a reduction or simplification in

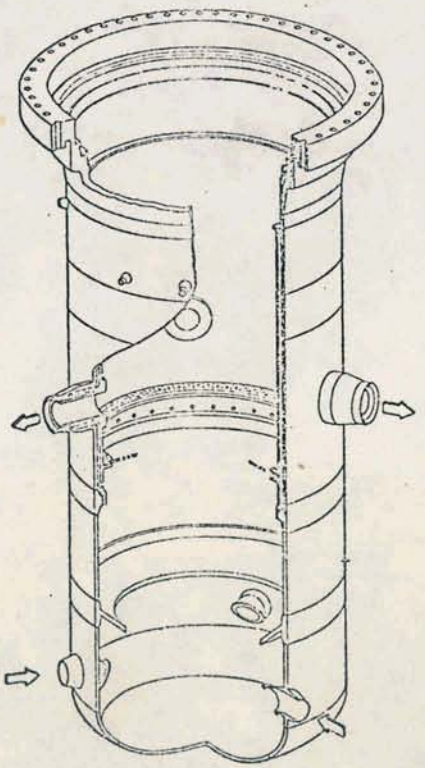

Figure 1

Reactor Vessel - Thermal Liner, CRBR

DISCLAIMER

the field equations can still result in a complex problem when three-dimensional geometries are considered. One such example is the dynamic analysis of coaxial cylinders which are found in reactor vessels such as the Clinch River Breeder Reactor (CRBR) illustrated in Figure 1. A vibration analysis of such a structure can still be difficult when the influence of the sodium is considered in concert with supports, contact points, nozzles, and piping attachments.

There have been many papers (4-17) that have treated such problems theoretically, however, with considerable simplification of the structure. A popular approach has been the finite element fluid pressure formulation, discussed in (18-22). The finite element method offers the ability to idealize the fluid and structure for arbitrary shapes which makes it a a popular technique. Another approach that has received much less attention is the finite element fluid displacement formulation as discussed in (23-25). In this paper, we will consider the small deflection vibration analysis utilizing the finite element displacement method. For a discussion of interfacing nonlinear solid-fluid analysis in vessels as shown in Figure 1, the reader is referred to Belytschko (26,27).

This paper will attempt to briefly explore through illustrative examples the advantages and disadvantages of the finite element displacement method to perform solid-fluid eigenvalue analyses.

2.0 THE FINITE ELEMENT METHOD

The finite element method concept is generally well known and covered in such texts as (28-31). We will only briefly review some of the fundamentals as they relate to the solid-fluid problem. Basically, the displacement approach assumes the fundamental "displacement" unknown at a node point of a fluid and structural element while the pressure method assumes a scalar unknown "pressure" at a node point of the fluid.

2.1 Finite element displacement method

In formulating the structural vibration problem using the finite element technique, the governing equations of motion can be expressed as

$$[M]\{\ddot{u}\} + [C]\{\dot{u}\} + [K]\{u\} = 0 \qquad (1)$$

where $[m]$, $[c]$, and $[k]$ are the assembled mass, damping, and the stiffness matrices for the idealized structure. $\{u\}$ corresponds to the vector of the dis-

placement components and a dot on $\{u\}$ denotes partial differentiation with respect to time. By applying the finite element displacement method to vibration problems with solid-fluid interaction effects, the mass matrix, $[m]$, is computed in the same manner as in the structural analysis. If the damping term is neglected, the only difference will be in the formulation of the stiffness matrix, $[k]$. The procedure for the formulation of the stiffness matrix for the fluid element is similar to that of the structural element except that a special constitutive law which relates the stress and strain by the material matrix $[G]$, must be defined for the fluid element.

In order to convert a standard structural element into a fluid element, we simply define the stress-strain material matrix $[G]$ (as discussed by Kalinowski (24), as follows:

$$G = K \begin{bmatrix} 1 & 1 & 1 & 0 & 0 & 0 \\ 1 & 1 & 1 & 0 & 0 & 0 \\ 1 & 1 & 1 & 0 & 0 & 0 \\ 0 & 0 & 0 & 0 & 0 & 0 \\ 0 & 0 & 0 & 0 & 0 & 0 \\ 0 & 0 & 0 & 0 & 0 & 0 \end{bmatrix} \qquad (2)$$

where K is the bulk modulus of the fluid.

We may note that the acoustic velocity (c) of fluid is calculated by

$$c = \sqrt{\frac{K}{\rho_f}} \quad \text{or} \quad K = c^2 \rho_f \qquad (3)$$

ρ_f = density of fluid

The advantage of this approach can be readily seen: any standard version of a finite element structural analysis program may be used for the solid-fluid interaction problem by introducing an appropriate material matrix, $[G]$. Now, the problem is reduced to solving an algebraic eigenvalue problem of equation (1) which yields the natural frequencies and the mode shapes of the combined solid and fluid structures.

2.2 Finite element pressure method

This approach uses the "pressure" unknown in the fluid domain while retaining the "displacement" unknown in the structural domain. The governing equations representing the structure are given in equation (1). The derivation of the governing equations in the fluid domain are based on the Navier-Stokes equations of fluid motion coupled with the continuity conditions. If we express the fluid pressure as a linear combination of a shape function, h_j, then

$$P = h_j p_j$$

where p represents the pressure at a grid point in the fluid. Neglecting the viscous terms, the governing equations in the fluid can be expressed with the boundary conditions, as

$$[Q] \{\ddot{p}\} + [H] \{p\} + \rho_f [B]^T \{\ddot{u}\} = 0 \qquad (4)$$

where ρ_f is the density of the fluid, Q and H are defined in the manner of reference (18).

The matrices $[Q]$, $[H]$ and the boundary matrix, $[B]$ can be expressed as functions of the shape functions, h_j. Note that the last term in equation (4) represents the effect of motion of the structures on the fluid. Similarly if we consider the effect of fluid motion

on the structure, the governing equation (1) of the structure must be modified to take into account the effect of fluid motion by adding a coupling term,

$$[M]\{\ddot{u}\} + [k]\{u\} - [B]\{p\} = 0 \qquad (5)$$

The damping term in equation (1) is again neglected. Equations (4) and (5) together provide a set of equations for the structure and another set of equations for the fluid. These two sets of equations are coupled by the boundary matrix term, [B]. Again the problem is reduced to a set of algebraic eigenvalue equations. The matrix generated from equations (4) and (5) will be non-symmetric due to the coupling terms, however, can be recast in a symmetric form with suitable operations discussed in reference (18).

The basic formulation of this type of fluid element follows the procedure as proposed by Everstine (19) etc. The basic assumption is that the fluid is treated as an acoustic medium and is to be compressible and inviscid. The fluid is further assumed to undergo only small amplitude motion and the "pressure" field within the medium satisfies the wave equation:

$$\nabla^2 p = \ddot{p}/c^2 \qquad (6)$$

The boundary conditions at the fluid-structure interface can be obtained from the momentum and continuity conditions. Two types of approaches, consistent and lumped methods have been suggested by Schroeder and Marcus (20), to model the fluid-structure interface.

For linear material, the Hooke's law can be written in terms of a symmetric material matrix, [G]. A necessary and sufficient condition for G to be isotropic and at the same time to satisfy the wave equation is

$$G = \rho_f c^2 \begin{bmatrix} 1 & -1 & -1 & 0 & 0 & 0 \\ -1 & 1 & -1 & 0 & 0 & 0 \\ -1 & -1 & 1 & 0 & 0 & 0 \\ 0 & 0 & 0 & 1 & 0 & 0 \\ 0 & 0 & 0 & 0 & 1 & 0 \\ 0 & 0 & 0 & 0 & 0 & 1 \end{bmatrix} \qquad (7)$$

To compute the stiffness matrix [k] of the fluid element, it is only necessary to model the fluid with standard elastic finite elements having material properties of G in equation (7).

By adopting the lumped approach in the fluid-structure interface, the influence of the structural motion on the pressure can be expressed as

$$F^p = (\rho_f c)^2 A \ddot{u}_n \qquad (8)$$

In other words, if the outward normal component of structural acceleration at a point is $\ddot{u}_n$, the effect on the fluid pressure is the "force" given by F^p. The inverse relationship (that of fluid pressure on the structural motion) is obtained by applying a normal force to the structural point by

$$F^s = PA \qquad (9)$$

The coupling terms $(\rho_f c)^2 A$ and A are precomputed in equations (8) and (9) at all solid-fluid interaction boundaries, and inserted in the stiffness and mass matrices for the solid-fluid system. These terms are inserted in the columns corresponding to the pressure of the fluid grid point and in rows corresponding to the structure displacements in the r direction

(assuming a cylindrical coordinate is used to model the solid-fluid system) of the structural grid point.

NASTRAN (32) provides the direct matrix input (DMIG) and thus no program modification is required to solve the solid-fluid interaction problem using the lumped techniques for the pressure analog fluid element as described above.

The Fourier approach assumes that the problem has an axial symmetry so that the "structural" model is defined by a set of fluid grid points in a plane that includes the axis of symmetry.

The pressure within a fluid element can be expanded in a Fourier series with respect to the azimuth coordinate, ϕ,

$$p(r,\phi,z) = p^{o} + \sum_{n=1}^{N} p^{n} \cos\phi n + \sum_{n=1}^{N} p^{n*} \sin n\phi \qquad (10)$$

The coefficients p^{o}, p^{n}, and p^{n*} are a function of position in a radial plane.

The motions of the coupled solid-fluid system need not be axisymmetric. The NASTRAN hydroelastic option provides a detailed description of this element. It allows the user to solve a wide variety of fluid problems having structural interaction.

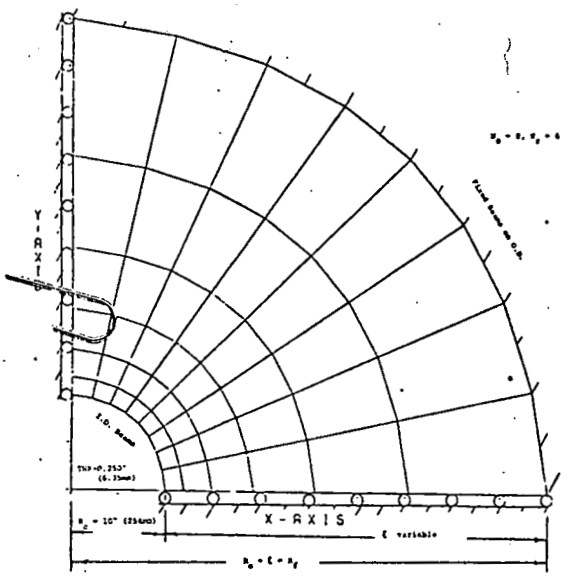

Figure 2

2-D Mesh of Infinite Cylinder Surrounded by Water

3.0 SAMPLE PROBLEMS COMPARING THE PRESSURE VS. DISPLACEMENT METHOD

3.1 The vibration of an infinitely long cylinder surrounded by water

The model described in Reference (20) consists of a carbon steel cylinder that has radius of 10 inches (250.4mm) to its centerline, a 0.25 inch (6.3mm) thickness, and water surrounding the outer surface. The fluid region is idealized by 2-D plane stress elements with the appropriate material matrix,[G] and

the cylindrical shell is modeled with beam elements. Figure 2 illustrates a quarter model used to evaluate the even mode and frequency results. Figure 3 illustrates the radial dimension and element refinement influence on convergence for the quadrilateral element with incompatable modes discussed by Wilson (33). We observe that acceptable accuracy is achieved for an outer fluid radius of about 30" (762mm) and a radial refinement of 5 to 6 elements (the modal response for ω_2 is illustrated in Figure 4). This

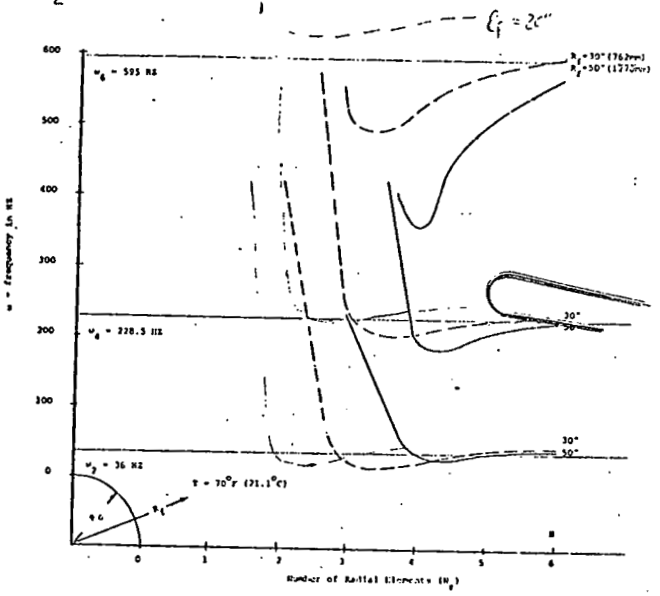

Figure 3

Element and Radial Dimension Convergence of The Q-5 Displacement Element

agrees with the NASTRAN quadrilateral pressure element data presented in Reference (20) which is summarized in Table 1. The displacement finite element and theoretical data is included for comparison.

Table 1

Method	Nθ	Nr	Outer Radius	frequency in Hz@ ω_2	ω_4	ω_6
Theoretical	-	-	∞	35.8	227.9	592.7
Displacement*	8	6	32.6 (828mm)	38.3	235.0	599.0
Pressure**						
a) consistent	8	6	"	37.5	248.6	671.8
b) consistent	16	12	"	36.4	233.3	615.8
c) lumped	8	6	"	36.9	236.5	618.2
d) lumped	16	12	"	36.2	230.3	601.0

* SAP 6 (Ref. 35) Nθ = number of circumferential elements

**NASTRAN Nr = number of radial elements

While the displacement method requires less computational time than the pressure method, the increase in the fluid mesh introduces increasing member of fluid frequencies for this and similar problems. This can be an undesirable feature of the method, but before we discuss this further-let's consider an instance where the fluid modes can be inhibited.

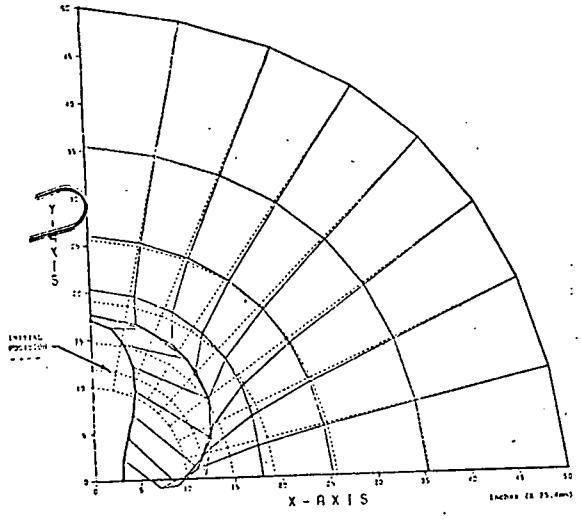

Figure 4

2-D Modal Displacement For
ω_2 = 35.9 HZ, Rf = 50" (1270mm)

3.2 The vibration of two thin co-axial cylinders with water-filled annulus

The radial dimensions to the cylinders centerlines discussed by Levin (8) are illustrated in Figure 5. The cylinders are made of carbon steel with ambient temperature H_2O in the annulus. Only one quarter of the structure is idealized by the finite element method; and only even modes are evaluated by specifying that $M_z \neq 0$ and no displacement normal to the plane of symmetry. Two finite element models are considered in this problem: 4 x 2 and 8 x 2 meshes. Both 2-D and 3-D elements are used. All 3-D elements are used with the boundary condition of plane strain in the Z direction.

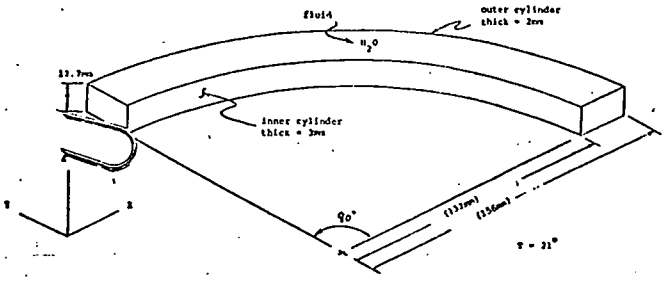

Figure 5

3-D Co-axial Cylinders With Water in the Annulus

The metal cylinders are idealized by using the 3-D plate element similar to Clough's (34). The 2-D idealizations of the cylinders are performed using beam elements. The fluid is represented by five types of elements:

a) 2-D displacement elements with incompatible modes (Q-5)/Reference (33)
b) 2-D pressure elements which are quadrilateral formed from static condensation of triangular elements/Reference (32)
c) 3-D displacement 8 node elements with incompatible modes (Q-11)/Reference (33)
d) 3-D pressure element (CHEXA) with 8 nodes available in NASTRAN. The interaction between the fluid and the structure is accomplished through the lumping technique.
e) 3-D Fourier pressure ring element (RINGFL) available in NASTRAN. The ring fluid elements are connected to the structure via (CFLUIDI) interface elements.

The out-of-phase 6th mode shape for ω_{06} = 355 Hz is illustrated in Figure 6. Table 2 provides a frequency comparison of the various methods cited with experimental data from Reference (8). The inphase modes are characterized by both cylinders oscillating together in a somewhat parallel fashion. The fluid also oscillates predominantly in the radial direction. The out-of-phase modes are characterized by the inner and outer cylinders moving in the radial direction but opposite at the same angular (θ) location. In this instance, the fluid motion is predominantly a tangent oscillation (to cylinder curved surface). As with the previous example, the two methods - compare favorably with the experimental data. The Q-5 2-D displacement solution provides the correct solid-fluid modes (no fluid modes/spurious modes were recorded). The Q-11 3-D displacement solution (8x2) provides the correct solid-fluid modes plus 3 additional spurious modes.

TABLE 2

COMPARISON OF FREQUENCIES (HZ)

DISPLACEMENT (FESAP) VS PRESSURE (NASTRAN) METHOD

Method	Mesh Dist.	Mode 2 I	Mode 2 o	Mode 4 I	Mode 4 o	Mode 6 I	Mode 6 o	Computer Time (CPU second)
* Displacement (2D Model QUS element)	8 x 2	74.7	25.4	294.7	111.6	968.4	332.1	1.4
** Displacement (3D Model Q-11 element)	8 x 2	78	32.5	420	307	1406	355	
* Displacement (3D Model Q-11 element)	4 x 2	79.2	32.7	446	325	836	418	2.2
**Fourier Pressure (3D Model Axi-fluid element)	4 x 2	80.1	29.6	529.7	353.4	1957.4	1337.8	240
**Pressure Analog (3D Model HEXA element)	4 x 2	89.6	33.96	473.4	309.4	1114.8	660.6	6.6
**Pressure Analog (2D Model QUSUM element)	4 x 2	85.8	31.6	453.8	185.5	1011.9	502.6	3.7
Experimental		80.0	30.0	340.0	305.0	750	330	

* FESAP
** NASTRAN

3.3 Advantages and disadvantages

a) Computational consideration - the advantage of using the displacement method is that any standard structural analysis program, such as SAP6, can be readily used. However, due to the sensitivity of the element formulation, shear viscosity, material properties and boundary conditions, a further discussion of these is provided in later sections. The pressure method has the advantage of requiring one (pressure) unknown per fluid point rather than three unknowns for the displacement method. However, the pressure method

has the disadvantage of generating nonsymmetric matrices (which through several matrix manipulations can be expressed in a symmetric form) in contrast to a symmetric form generated by the displacement method. The computer time for the Fourier pressure method is approximately ten times that of the 3-D pressure analog method. This is due to the fact that the NASTRAN Fourier pressure method uses the complex eigenvalue search routine. The computer cost between the displacement method and the 3-D pressure analog method is comparable, but the pressure method is several times more expensive. The CPU seconds given in Table 2 shows a qualitative comparison since the mesh is too small to show an absolute quantitative comparison.

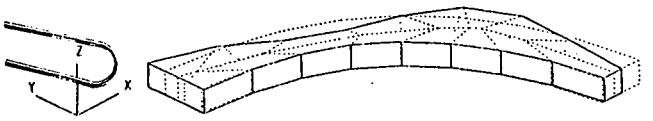

Figure 6

3-D Modal Displacement of Co-axial Cylinders for ω_{06} = 355 HZ

b) Spurious Frequencies - The additional spurious fluid modes generated from the displacement fluid element creates problems when only the structural modes are of interest. From this point of view, the pressure approach appears to be more attractive provided that the analyst can correctly predict the frequency range to be searched within NASTRAN. Even with a proper range of frequency specified, it is possible to generate additional spurious frequencies when using the NASTRAN pressure method (either the pressure analog or Fourier pressure method). There are several ways to determine which frequencies are actually fluid or structural frequencies rather than fluid only frequencies. The easiest way is to plot the mode shapes. For the "fluid-only" modes, the structure will show very little, if any, relative displacement. For the fluid-structural modes the structure as well as the fluid will have significant relative displacements. A second way is to completely fix the structure and make a second run. This will yield only fluid frequencies. By comparing the results of the "fluid-only" run with the normal run, the common frequencies can be identified as fluid frequencies. This procedure is not fool-proof. A third alternative is to examine the mode displacement data from the full run to determine which frequencies have the larger structural values. Generally, the structural frequencies are dominant. This procedure is subject to significant judgement at times and selective mode shapes should be plotted for verification. If a range of fluid frequencies is known to exist, the eigenvalue shift may be used to eliminate them. For example, the first few frequencies found for the 3.1 problem are fluid frequencies. By requesting the truncation of frequencies below 30 HZ, the solution of these fluid frequencies is omitted. Finally, the fluid frequencies may be filtered from the solution by limiting those modes with relatively low internal

energy within the structural domain from the total solution.

4.0 THE DISPLACEMENT METHOD

From the previous two illustrative problems, it is evident that the desirable structural frequencies with interacting fluid can be obtained by the displacement method. In this section, we will explore further the displacement method with respect to:

- effect of element formulation
- influence of shear viscosity
- effect of mesh distribution, geometry
- effect of boundary conditions
- study of integration order, plane stress, plane strain

4.1 Effect of element formulation for the displacement method

A question that problem 3.2 raises is what is the function of the fluid element formulation in characterizing the inphase and out-of-phase modes of the co-axial cylinders? We provide a limited comparison in this paper by choosing a 3-D 8 node element as the base and vary the stiffness characteristics. The five formulations considered are:

Table 3

Element identity	Descriptions
a. Q-8	compatible mode
b. Q-8/one point integration	compatible mode using one point integration
c. Q-9	incompatible mode with respect to centroid in one(1) degree of freedom
d. Q-11	incompatible mode with respect to centroid in three(3) degree of freedom
e. Q-14	incompatible mode with respect to centroid of six(6) surfaces

For the Q-8, the displacement approximations are assumed to be

$$u_j = h_i u_{ji} \tag{11}$$

where in indicial notation $j = 1,2,3$ (coordinate frame) and $i = 1$ to 8 (nodal reference)

$$h_1 = 1/8\ RST \qquad h_5 = 1/8\ RS\bar{T}$$
$$h_2 = 1/8\ \bar{R}ST \qquad h_6 = 1/8\ \bar{R}S\bar{T}$$
$$h_3 = 1/8\ \bar{R}\bar{S}T \qquad h_7 = 1/8\ \bar{R}\bar{S}\bar{T}$$
$$h_4 = 1/8\ R\bar{S}T \qquad h_8 = 1/8\ R\bar{S}\bar{T}$$

where $R = (1 + r)$, $S = (1 + s)$, $T = (1 + t)$
$\bar{R} = (1 - r)$, $\bar{S} = (1 - s)$, $\bar{T} = (1 - t)$

and r,s,t are the local coordinate frame. For a single point integration the same element is used with an adjustment of the weight function and integration points.

For the Q-9 element, equation (11) takes the form

$$u_j = h_i u_{ji} + h_9 \alpha_j \tag{12}$$

where $h_9 = \bar{R}R\bar{S}S\bar{T}T$

The Q-11 displacement polynomial is written as

$$u_j = h_i u_{ji} + h_k \alpha_{jk} \qquad (13)$$

where k = 9,10,11

$h_9 = R\bar{R}$, $h_{10} = S\bar{S}$, and $h_{11} = T\bar{T}$

For the Q-14 element equation (11) is rewritten as

$$u_j = h_i u_{ji} + h_l \alpha_{jl}$$

where l = 9,10,11,12,13,14

and

$h_9 = R\bar{R}S\bar{S}T$ $\qquad$ $h_{12} = \bar{R}S\bar{S}T\bar{T}$

$h_{10} = R\bar{R}S\bar{S}\bar{T}$ $\qquad$ $h_{13} = \bar{R}RST\bar{T}$

$h_{11} = RS\bar{S}T\bar{T}$ $\qquad$ $h_{14} = \bar{R}R\bar{S}T\bar{T}$

The centroids of each bending coefficient is located at six element faces.

TABLE 4

COMPARISON OF FREQUENCIES WITH VARIOUS ELEMENT FORMULATION USING DISPLACEMENT METHOD

Element Formulation	Mode 3		Mode 4		Mode 6	
	ψ	φ	ψ	φ	ψ	φ
Q-8	104.8	--	481.3	--	934	--
Q-8 (One Point Integration)	82.6	25.4	446	170.7	1074	574
Q-9	89.2	--	446	--	1358	--
Q-11	82.6	25.4	446	170.6	1074	574
Q-14	82.1	--	515	--	1448	--
Experimental	50.0	10.0	340	105	750	330

Note: All frequencies are computed using shear coefficient = 0.319

Thickness of inner & outer cylinders = .118"

ψ = inplane mode $\qquad$ φ = out-of-plane mode

Table 4 provides a comparison of frequencies obtained for the problem discussed in section 3.2 using the element formulations in Table 3 with an 8x2 mesh. Q-8 is an element without incompatible modes. Table 4 indicates that both Q-11 and Q-8 (with one point integration) provide acceptable results as compared with the experimental results by Levin(8). Element types Q-8, Q-9 and Q-14 do produce the inphase modes, but the lowest three out-of-phase modes are missing. Between Q-11 and the one point integration Q-8, the latter requires less computer time to formulate the element stiffness but at the same time it generates additional spurious fluid modes which need to be removed for structural response spectrum analysis. It should be pointed out that with a smaller μ (say 0.0319 - see Table 2), Q-11 will provide a better comparison with the experimental data. The influence of the element formulation with respect to shear stiffness and its importance to solving many solid-fluid interaction problems can be further illustrated by the following example.

Consider a simple rectangular container with the dimensions AxB [4" (101.6mm) x 25" (635mm)] whose walls are rigid and bound water.

The properties of water at $70^{o}F(21.1^{o}C)$ are:

K (bulk modulus) = 319,000 psi (219.9MPa)
ν (poisson's ratio) = 0.5
ρ (density) = 0.03605 # / in^3 (0.5775 Kg/M^3)

From the fundamental mechanics of vibration, we can show that

Dilatational Modes: $$\omega = c\sqrt{\left(\frac{m\pi}{A}\right)^2 \left(\frac{m\pi}{B}\right)^2} \qquad (14)$$

Rotational Modes: $\omega = 0.0$
;m,n = 1,2,3 (15)

Only motion tangent to the rigid wall is permitted at the boundaries. The remaining nodes have two degrees of freedom. Two types of elements are used in this illustrative problem: (1) the NASTRAN 2-D quadrilateral formed by triangular elements (Q-3) and (2) the Wilson 2-D Q-5 incompatible mode element. Finite element meshes (3 x 19), (4 x 25), (5 x 31), to (8 x 50) (Number of elements in the A dimension X Number of elements in B dimension) are constructed for this study and μ = 0.0. The frequency response of the Q-3 and Q-5 are illustrated in Figure 7a. As the mesh is refined, we observe the convergence of the Q-3 solution for the first rotational frequency to the exact value of zero. The Q-5 element solution (illustrated in Figure 7) shows that the coarse mesh results in all permissible rotational modes (for this mesh) falling below 58 HZ. The first rotational frequency is 0.77 HZ for this Q-5 solution.

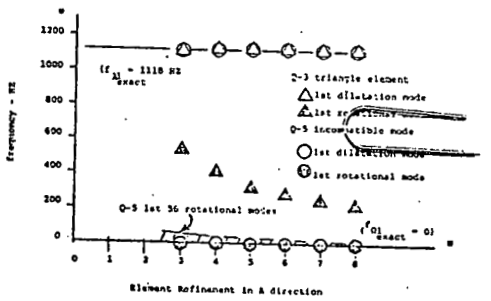

Figure 7a
Dilatation (f_λ) and Rotation (f_Ω)
Frequency vs Element Refinement

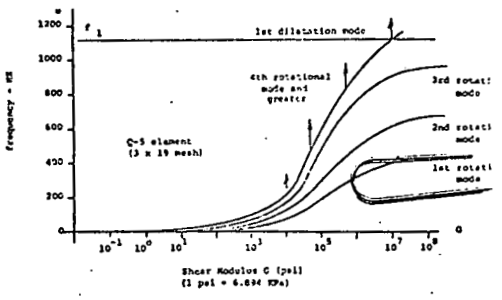

Figure 7b
Rotational Frequency (f_Ω) vs Shear Modulus (G)

Our results show that the rotational modes of the finite element tend to zero and zero pressure is associated with them for the μ and boundary conditions chosen. An important point is the ability of

the incompatible mode element (Q-5) to achieve zero for the more refined meshes. This is a consequence of the shear condition assumed with respect to the shape function for the Q-5 element, i.e., local shear stiffness is zero in a bending mode. We would expect that if the vorticity ($\Omega = 2\bar{W}$) were zero where

$$\bar{W}_i = \tfrac{1}{2} E_{ijk} \bar{W}_{jk} \quad \text{and} \quad \begin{matrix} i = x, y, z \\ j = x, y, z \\ k = x, y, z \end{matrix}$$

then the rotational modes are not permissable.

In order to obtain some measure of irrotationality, let's consider the fact that in a two dimensional shear flow, we have

$$u = f(y),\ v = 0,\ w = 0$$

$$\Omega_z = 2\bar{W}_z = v,x - u,y = u,y = f(y),y.$$

If we remember that shear is defined as

$$\gamma_{xy} = v,x + u,y = u,y = f(y),y$$

we can influence the irrotationality of the field by modifying μ or G. As shear stiffness approaches infinity the shear strains become zero.

In Figure 7b, the response of the 3 x 19 element mesh for variable G or μ using the Q-5 element is illustrated. The first dilatation mode is unaffected but the 4th through 56th rotational frequencies become greater than the first dilatation frequency (1118 HZ) @ $\mu \to 10^7$ psi. The 1st, 2nd and 3rd rotational frequencies appear to have converged to some value below 1118 HZ.

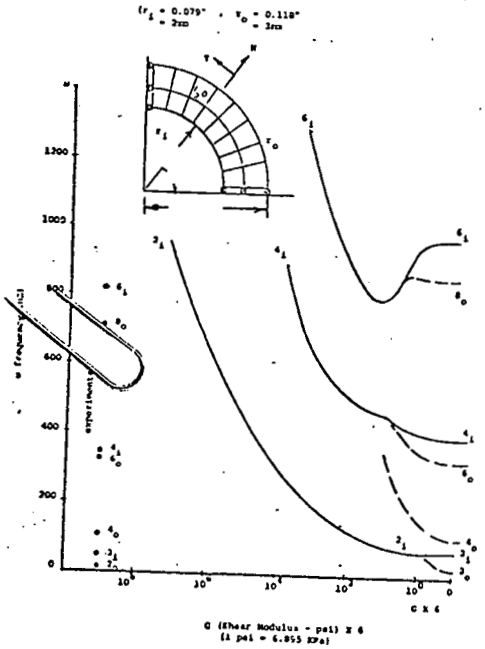

Figure 8

Inphase and Out-of-phase Frequency vs G For Co-axial Cylinders

For a more coarse mesh, the 1st, 2nd and 3rd rotational frequencies increase above 1118 HZ. Our data indicates that the boundaries and modeling assumptions tend to lead to a combination of compressability and rotationality for this particular mesh. This study shows that irrotationality ($\Omega = 0$) can eliminate rotational frequencies of the fluid when they are undesirable and that a no pressure state is associated with these frequencies.

4.2 Influence of shear viscosity

Again, we consider the vibration of the co-axial cylinders of infinite length connected by a fluid gap discussed in section 3.2. This is modeled by the Q-5 Wilson 2-D element with a 2 x 8 mesh illustrated within Figure 14.

Because of our choice of boundaries and a 90^{o} model, only even modes of vibration are evaluated. For large shear coefficient values, only inphase frequencies (2_i, 4_i, 6_i) are present (see Figure 8).

The irrotational or circulation modes (Γ) are inhibited in 2-D problems by stiffening or increasing the G or μ. In Figure 8, we see that as $\mu \to 0$ the out-of-phase frequencies (2_o, 4_o, 6_o and 8_o) appear. The finite element solutions compare quite well to the experimental data for G = 0. No spurious frequencies were encountered.

A similar evaluation was repeated using the 3-D Q-11 fluid element. The results were comparable, but some spurious frequencies were encountered and easily identified.

4.3 Assessment of mesh, boundaries, and other parameters

Risking the possibility of over generalizing because of space limitations, we will summarize the effect of some of the parameters in the type of solid-fluid analyses we have presented rather than present the tabular numerical data. Using the flexible co-axial cylinder problem with annular fluid we find:

- mesh refinement: a slight increase in accuracy with a significant increase in rotational fluid frequencies.
- integration order: an increase in integration order does not have a measurable influence. This may not be the case for large aspect ratio elements.
- free displacement surface versus plane strain (plane strain is effectuated by constraining Z displacements at one evaluation or side of the thickness of the fluid) more spurious fluid frequencies are encountered by the free surface than plane strain.
- element compatibility: there is bending stress associated with pure shear or with pure bending there is shear associated with this action. As a consequence of this, rotational modes are inhibited. Only the inphase modes are determined by this option and no spurious fluid frequencies. Inclusion of incompatibility modes results in the correct inphase and out-of-phase frequencies with spurious shell and fluid modes.

- shear viscosity (μ or G): $\mu \approx 0$ for out-of-phase modes

- fluid mass: for thin gaps between the inner and outer cylinders, the inphase frequencies are less sensitive than out-of-phase modes. As fluid density (ρ)$\neq$0 the out-of-phase modal frequencies increase.

- beam or boundary elements: the use of beam elements or boundary elements interfacing between the fluid and structure may or may not be necessary. For the co-axial cylinder problem, boundary elements did not improve accuracy versus direct attachment of the fluid to the structure. In this problem, the acoustic frequencies were unimportant. In the rectangular container problem, direct attachment of the fluid to the structure will inhibit the dilatation modes.

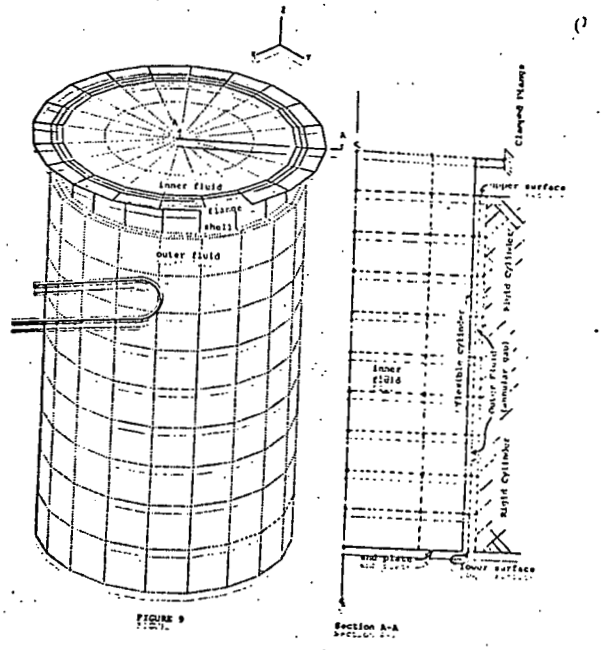

Figure 9

3-D Mesh of Co-axial Cantilever and Rigid Cylinders Filled With Water

5.0 3-D SOLUTION OF SOLID-FLUID INTERACTION PROBLEMS

In order to illustrate the use of the 3-D finite element displacement method to solve finite co-axial cylinder vibration problems in the presence of a fluid (such as found in nuclear reactors), let's consider the problem of a flexible carbon steel cylinder suspended by a flange and capped at the other end, discussed in Reference (11). The cylinder is immersed in 70°F(21.1°C) H_2O and has a 1 inch (25.4mm) radial gap between it and an outer rigid cylinder. The dimensions of the flexible cylinder are: 0.125" (3.175mm) thick shell, 22" (558.8mm) O.D. x 44" (1117.6mm) length of the cylinder, 0.5" (12.7mm) end plate, and a flange with a 1" (25.4mm) thickness x 21.75" (552.45mm) I.D. x 27.5" (698.5mm) O.D. - bolt circle. The 3-D mesh using the Q-11 element for fluid and the shell element previously discussed for the structure, is illustrated in Figure 9 and itemized in

Table 5.

Table 5

3-D Solid-Fluid Cantilever Cylinder

	No. of Elements	Element
cylinder	300	Q-19 Plate (Ref. 34)
inner water	400	Q-8 compatible (Table 3)
outer water	400	Q-11 incompatible (Table 3)
total	1100	

The outer fluid nodes are fixed to simulate the rigid outer cylinder, and the upper surface fluid nodes (see Figure 9) in the annulus are constrained to no displacement in the Z direction. A resevoir of H_2O is under the end plate of the cylinder, hence the lower surface annular fluid is not constrained. The inner fluid surface is also free. A comparison of the frequency results from experimental tests and the finite element displacement method are provided in Table 6 for the following cases: no water present, water in the inner cylinder, and water in the inner and outer cylinders. The results agree quite well. The only discrepancy is the evaluation by finite element of some modes that were ill defined or difficult to locate experimentally.

Table 6

Frequency (HZ) Comparison

Mode (n,m)	Experimental (Support Stand)	Analytical Model
Cylinder in air:		
1,0	33.8	46.6
2,1	331	359.8
3,1	205	209.3
4,1	196	196.7
5,1	255	261.6
CPU = 124 sec. (CDC 7600)		
Inner cylinder filled with H_2O:		
1,0	30.3	26.1, 105.1
2,1	NR(Could not locate)	110.3
3,1	103	119.3
4,1	106	131.0
5,1	145, 148	144.1
CPU = 293 sec. (CDC 7600)		
Inner and outer cylinder filled with H_2O:		
4,0	NR	11.0, 24.8
1,0	30.5*	29.6
1,0	30.5*	44.4
2,1	64.4	69.7
3,1	53.5	52.8
4,1	59.7	61.4
5,1	89.4	93.7
CPU = 477 sec. (CDC 7600)		

n = circumferential
m = longitudinal
* = ill defined

6.0 DISCUSSION AND CONCLUSION

In this paper, we have shown through comparison to experimental, theoretical, and other finite element formulations that the finite element displacement method can solve accurately and economically a certain class of solid-fluid eigenvalue problems. The problems considered are small displacements in the absence of viscous damping and are 2-D and 3-D in nature. A problem analyzed in detail by the authors using the finite displacement method, but not presented here because of space limitations, is the analysis of finite co-axial flexible cylinders connected by a fluid filled annulus (as discussed in Reference 16). In this study the advantages of the finite element method (in particular the displacement formulation) is apparent in that a large structure consisting of the cylinders, support flanges, fluid and other experimental boundaries could be modeled to yield good correlation to experimental data. The ability to handle large problems with standard structural programs is the key advantage of the displacement fluid method. The greatest obstacle is the inability of the analyst to inhibit those rotational degrees of freedom that are unnecessary to his fluid-structure vibration problem. With judicious use of element formulation, boundary conditions and modeling, the displacement finite element method can be successfully used to predict solid-fluid response to vibration and seismic loading.

7.0 ACKNOWLEDGMENT

The authors would like to thank M. E. Fox, J. R. Woolsey and D. A. McKinley for their assistance in generating some of the finite element results and T. L. Jursik for her assistance in preparing this manuscript. The authors would also like to thank the Clinch River Breeder Reactor Program for the partial funding of this study.

8.0 REFERENCES

1. J. E. Greenspan, "Fluid-Solid Interaction", ASME Symposium, 1967.

2. M. K. Au-Yang, and S. J. Brown, "Fluid Structure Interaction Phenomena in Pressure Vessel and Piping Systems", ASME-PVP-PB-026, (1977).

3. T. Belytschko, and T. L. Geers, "Computational Methods for Fluid-Structure Interaction Problems" ASME-AMD-vol. 26, (1977).

4. R. J. Fritz, "The Effect of Liquids on the Dynamic Motions of Immersed Solids", Journal of Engineering for Industry, Feb., 1972.

5. D. Krajcinovic, "Vibration of Two Co-axial Cylindrical Shells Containing Fluid", Nuclear Engineering and Design 30 (1974).

6. G. R. Sharp and W. A. Wenzel, "Hydrodynamic Mass Matrix For A Multi-Bodied System", WAPD-TM-1087, Bettis Atomic Power Life, 1973 (73-DET-121/ASME).

7. S. S. Chen, "Free Vibration of A Coupled Fluid/Structural System", Journal of Sound and Vibration 21 (1975).

8. L. Levin and D. Milan, "Coupled Breathing Vibrations of Two Thin Cylindrical Co-axial Shells in

Fluid", Vib. Problems in Industry, Intn'l Symposium, Keswick, England, 1973.

9. G. Bowers and G. Horvay, "Beam Modes of Vibration of a Thin Cylindrical Shell Flexibly Supported and Immersed in Water Inside of a Co-axial Cylindrical Container of Slightly Larger Radius", Nuclear Engnr. and Design 26 (1974).

10. R. J. Fritz, "The Effects of a Annular Fluid on the Vibrations of a Long Rotor, Part 1 & 2 - Theory and Test, Journal of Basic Engineering, Vol. 92, 1970.

11. M. K. Au-Yang, "Generalized Hydrodynamic Mass for Beam Mode Vibration of Cylinders Coupled by Fluid Gap", TRG-76-7 (Babcock & Wilcox Co. Report, 1976).

12. G. Bowers and G. Horvay, "Forced Vibration of a Shell Inside a Narrow Water Annulus", Nuclear Engineering and Design 34 (1975).

13. M. K. Au-Yang, "Free Vibration of Fluid - Coupled Co-axial Cylindrical Shells of Different Lengths", Journal of Applied Mechanics, Vol. 98, (1976).

14. M. K. Au-Yang, "Response of Reactor Internals to Fluctuating Pressure Forces", Nuclear Engineering and Design 35 (1975).

15. W. J. Stokey and R. J. Scavuzzo, "Normal Mode Solution of Fluid Coupled Concentric Cylindrical Vessels", ASME-77-PVP-37.

16. M. K. Au-Yang and D. A. Skinner, "Effect of Hydrodynamic Mass Coupling on the Response of a Nuclear Reactor to Ground Acceleration", 4th Intn'l Conference on SMIRT, 1977.

17. P. Turula and T. M. Mulcahy, "Computer Modeling of Flow Induced In-Reactor Vibrations", ASME-Power Division Journal - July 1977.

18. O. C. Zienkiewicz and R. E. Newton, "Coupled Vibrations of a Structure Submerged in a Compressible Fluid," Intn'l Symposium on Finite Element Techniques, University of Stuttgart, Germany, 1969.

19. G. Everstine, E. Schroeder, M. Marcus, "The Dynamic Analysis of Submerged Structures," NASTRAN Symposium, NASA TMX-3278, Sept. 1975.

20. E. Schroeder and M. Marcus, "Finite Element Solution of Fluid - Structure Interaction Problems," 46th Shock and Vibration Symposium, October, 1975.

21. S. Levy and J. P. D. Wilkinson, "Calculation of Added Water Mass Effects For Reactor System Components," 3rd International SMIRT (1975).

22. H. Chung, P. Turula, T. M. Mulcahy, and J. A. Jendrzijczyk, "Analysis of a Cylindrical Shell Vibrating in a Cylindrical Fluid Region", ANL-76-48 (Argonne Nat'l Lab Report), (1976).

23. E. L. Wilson, "Finite Elements for Foundations, Joints and Fluids," International Symposium on Mechanical Methods in Soil Mechanics and Rock Mechanics, Univ. of Karlruhe, Germany, Sept. 15-19, 1975.

24. A. J. Kalinowski, "Fluid Structure Interaction Solutions Using Finite Elements," NSR&D, Proceedings of the 5th NAVY-NASTRAN Colloquium, CMD-32-74, 1974.

25. H. V. Akay, N. Akkas, and C. Vilnaz, "Analysis of Solid-Fluid Interaction Problems with SAPIV", SAP Users Conference, June 22-23, 1977.

26. T. Belytschko and J. M. Kennedy, "A Fluid-Structure Finite Element Method For The Analysis of Reactor Safety Problems," Nuclear Engineering and Design 38 (1976).

27. T. Belytschko, "Methods and Programs for Analysis of Fluid-Structure Systems", Nuclear Engineering and Design 42 (1977).

28. O. C. Zienkiewicz, "The Finite Element Method in Engineering Science," McGraw-Hill, 1971.

29. R. A. Gallagher, "Finite Element Analysis," Prentice Hall, Inc. Englewood Cliffs, NJ., 1975.

30. K. J. Bathe, and E. L. Wilson, "Numerical Methods in Finite Element Analysis," Prentice Hall, Inc., Englewood Cliffs, NJ, 1975.

31. J. J. Connor and C. A. Brebbia, "Finite Element Techniques for Fluid-Flow", Newnes-Butterworths, London (1976).

32. The National Aeronautics and Space Administration, NASTRAN, NASTRAN Theoretical Manual, NASA-SP-221 (01).

33. S. J. Fenves, N. Perronne, A. R. Robinson, and Schnolrich editors, E. L. Wilson et al, "Incompatible Displacement Models," from Numerical and Computer Methods in Structural Mechanics, Academic Press, 1973.

34. R. W. Clough, "A Refined Quadrilateral Element For Analysis of Plate Bending," AFFDL-TR-68-150, 1968.

35. SAP6, "A Structural Analysis Program for Static and Dynamic Analysis," User's Manual, November, 1977, SAP User's Group, University of Southern California.

TABLE 2

COMPARISON OF FREQUENCIES (HZ)

DISPLACEMENT (FESAP) VS PRESSURE (NASTRAN) METHOD

Method	Mesh Dist.	Mode 2		Mode 4		Mode 6		Computer Time (CPU second)
		I	O	I	O	I	O	
* Displacement (2D Model QM5 element)	8 x 2	74.2	25.4	394.7	111.6	968.4	339.1	1.4
* Displacement (3D Model Q-11 element)	8 x 2	78	12.5	420	107	1006	355	10
* Displacement (3D Model Q-11 element)	4 x 2	79.2	12.7	446	125	936	418	2.2
**Fourier Pressure (3D Model Axi-fluid element)	4 x 2	90.1	24.6	529.7	253.4	1857.4	1337.8	140
**Pressure Analog (3D Model HEXA element)	4 x 2	89.6	22.96	473.4	209.4	1114.8	660.6	8.6
**Pressure Analog (2D Model CQDMEM element)	4 x 2	85.8	21.6	453.8	185.5	1011.9	502.6	3.7
Experimental		50.0	10.0	340.0	105.0	750	330	

* SAP6
**NASTRAN
I = inphase modes
O = out-of-phase modes

TABLE 4

COMPARISON OF FREQUENCIES WITH VARIOUS ELEMENT FORMULATION

USING DISPLACEMENT METHOD

Element Formulation	Mode 2		Mode 4		Mode 6	
	I	O	I	O	I	O
Q-8	104.8	--	481.3	--	934	--
Q-8 (One Point Integration)	82.6	25.4	446	107.7	1074	574
Q-9	89.2	--	444	--	1158	--
Q-11	82.6	25.4	446	107.6	1074	574
Q-14	82.1	--	515	--	1448	--
Experimental	50.0	10.0	340	105	750	330

Note: All frequencies are computed using shear coefficient = 0.319 psi (7.213 KPa)

Thickness of inner & outer cylinders = .118(3mm)

I = inphase mode O = out-of-phase mode

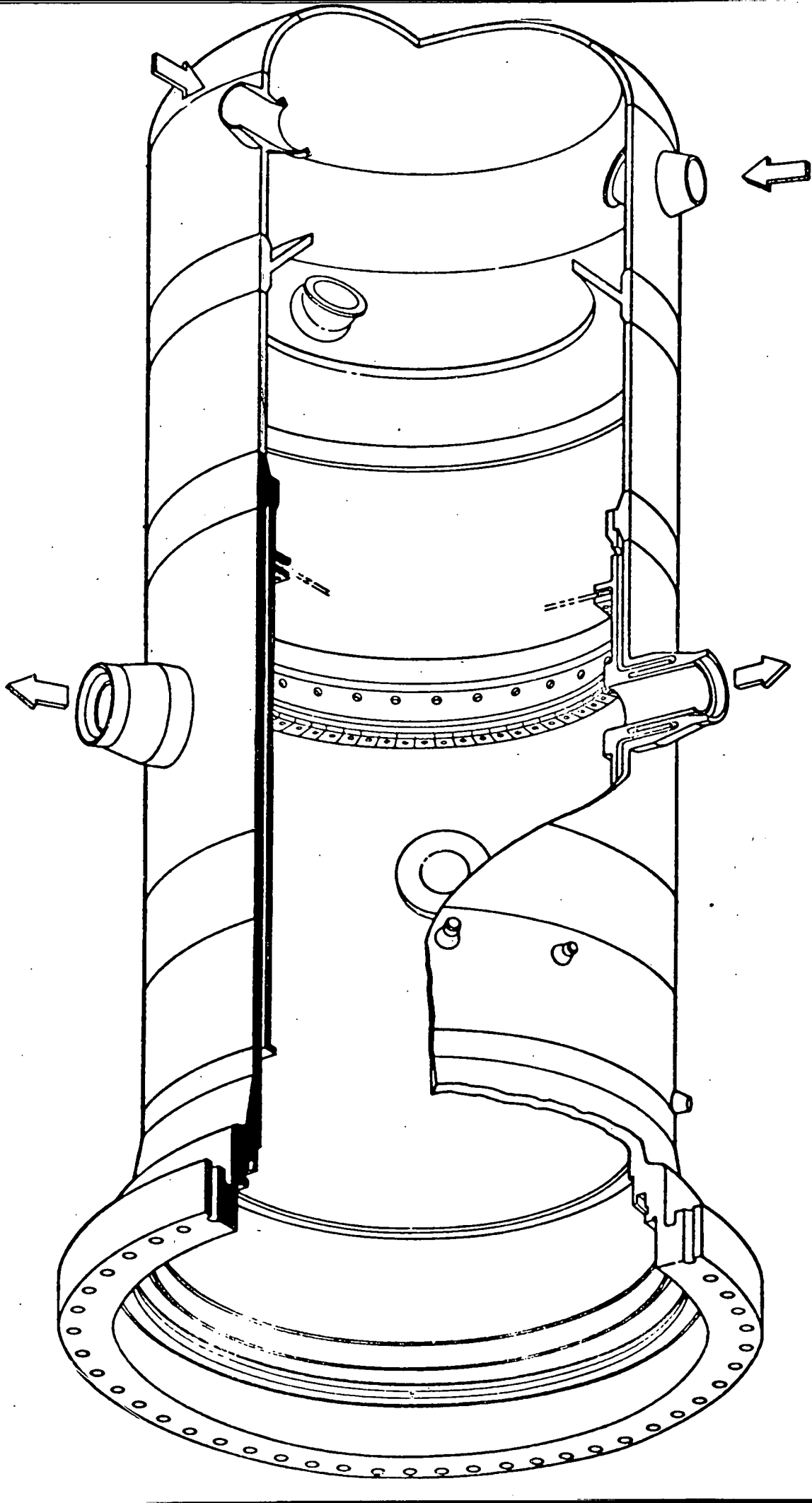

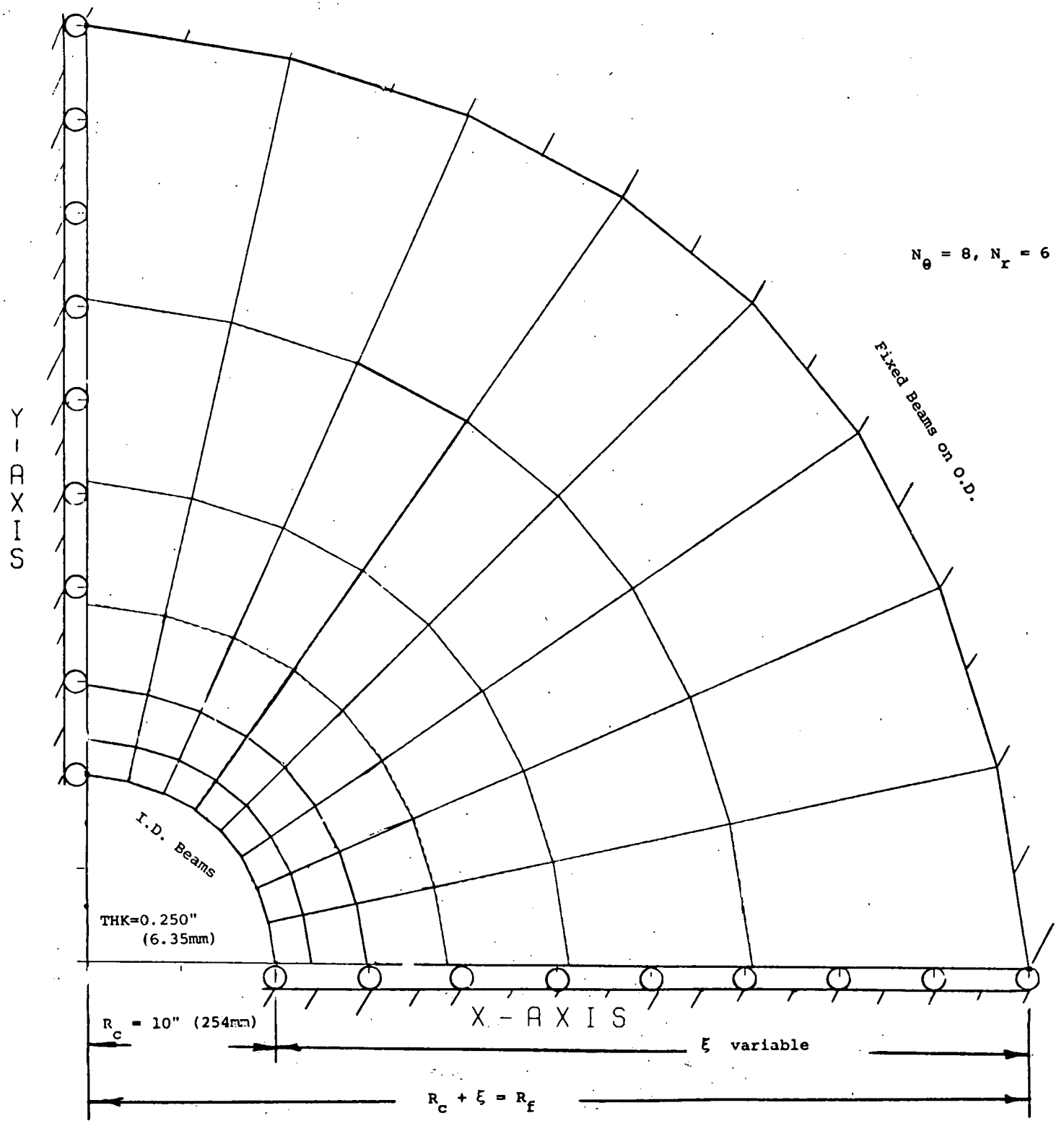
$N_\theta = 8$, $N_r = 6$
Fixed Beams on O.D.
Y-AXIS
I.D. Beams
THK=0.250"
(6.35mm)
X-AXIS
R_c = 10" (254mm)
ξ variable
$R_c + \xi = R_f$

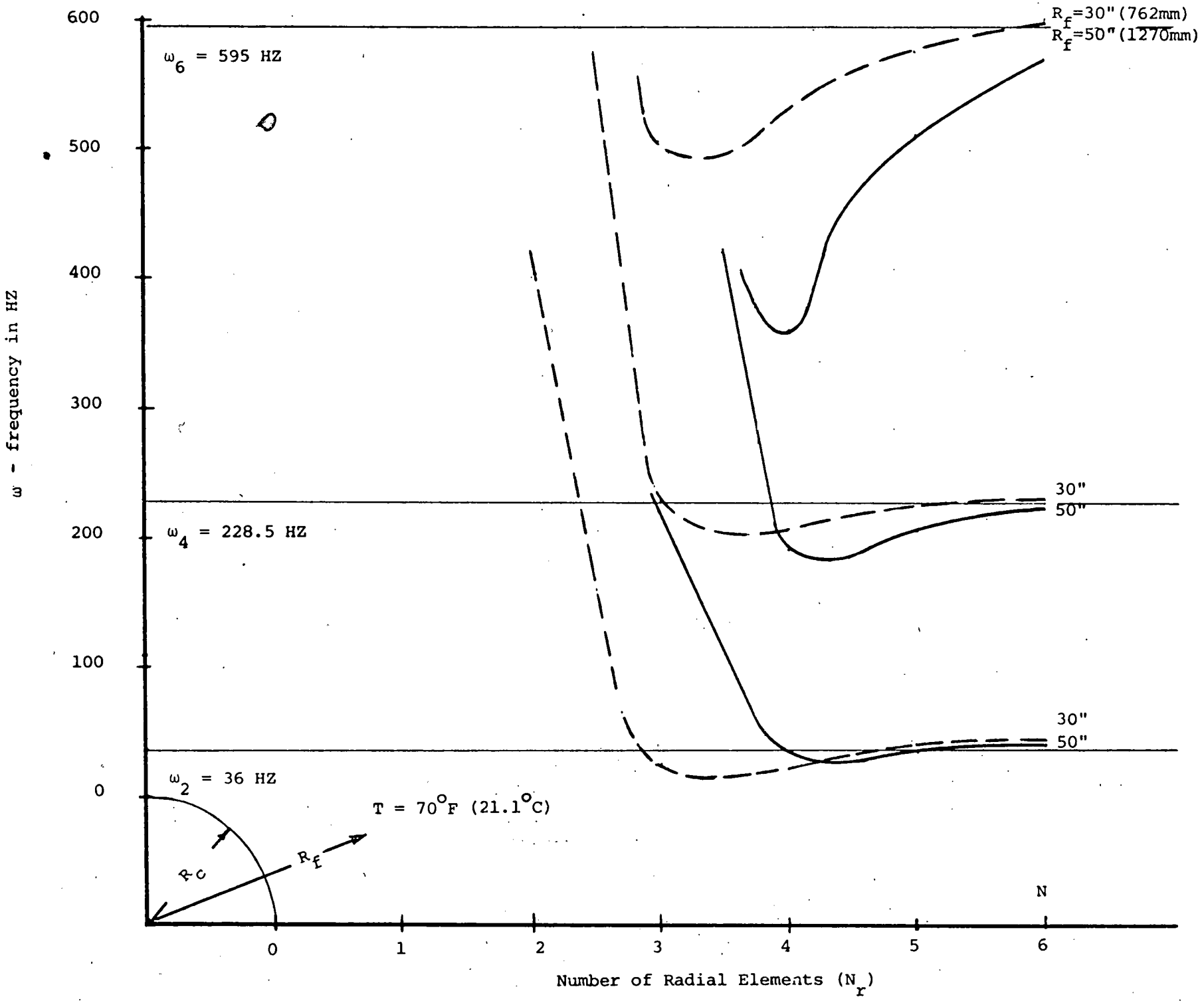
600
500
400
300
200
100
0
ω - frequency in HZ
ω_6 = 595 HZ
ω_4 = 228.5 HZ
ω_2 = 36 HZ
R_f=30" (762mm)
R_f=50" (1270mm)
30"
50"
30"
50"
T = 70°F (21.1°C)
R_f
N
0
1
2
3
4
5
6
Number of Radial Elements (N_r)

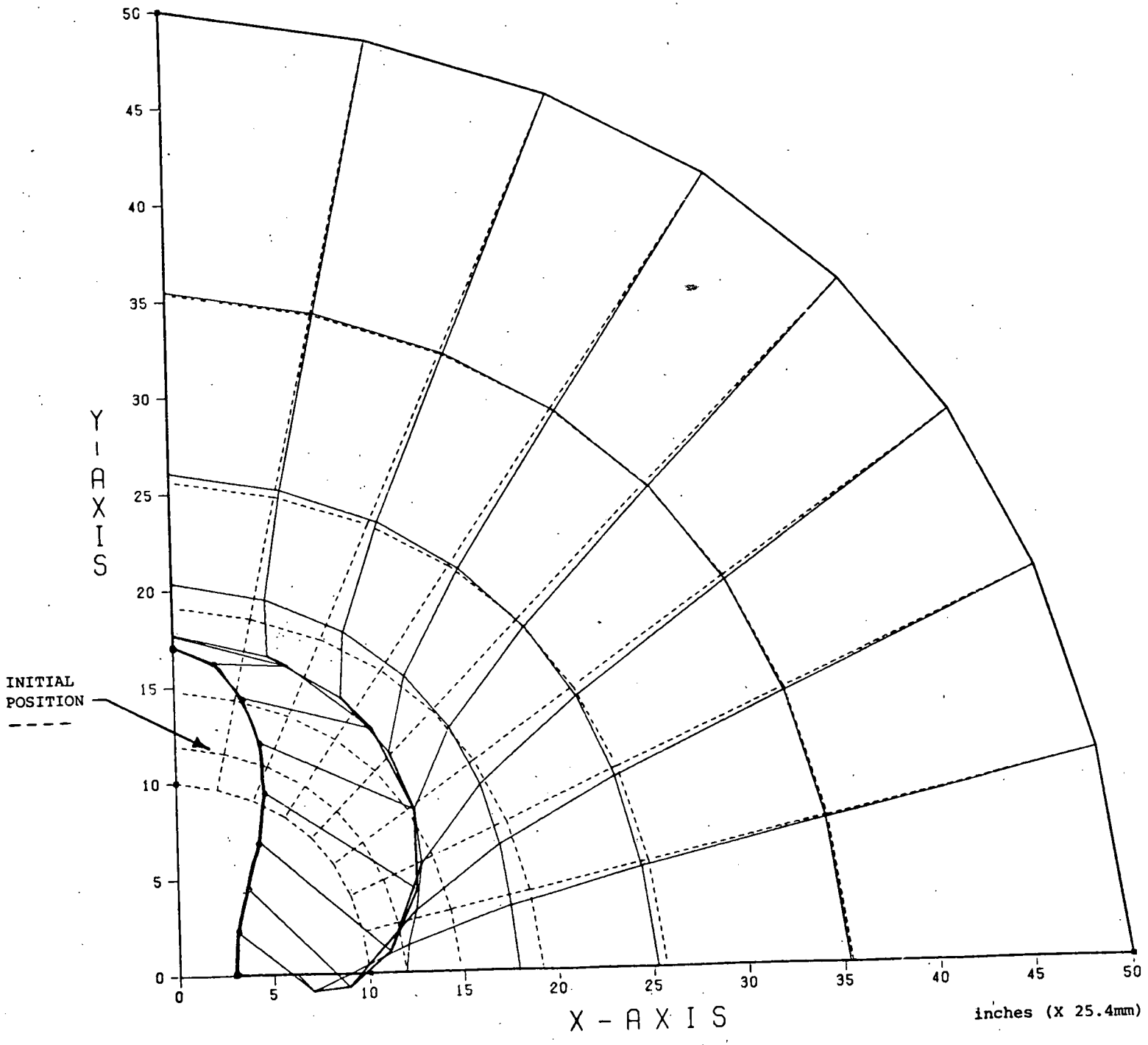
50
45
40
35
30
25
20
15
10
5
0
Y-AXIS
INITIAL
POSITION
0
5
10
15
20
25
30
35
40
45
50
X - A X I S
inches (X 25.4mm)

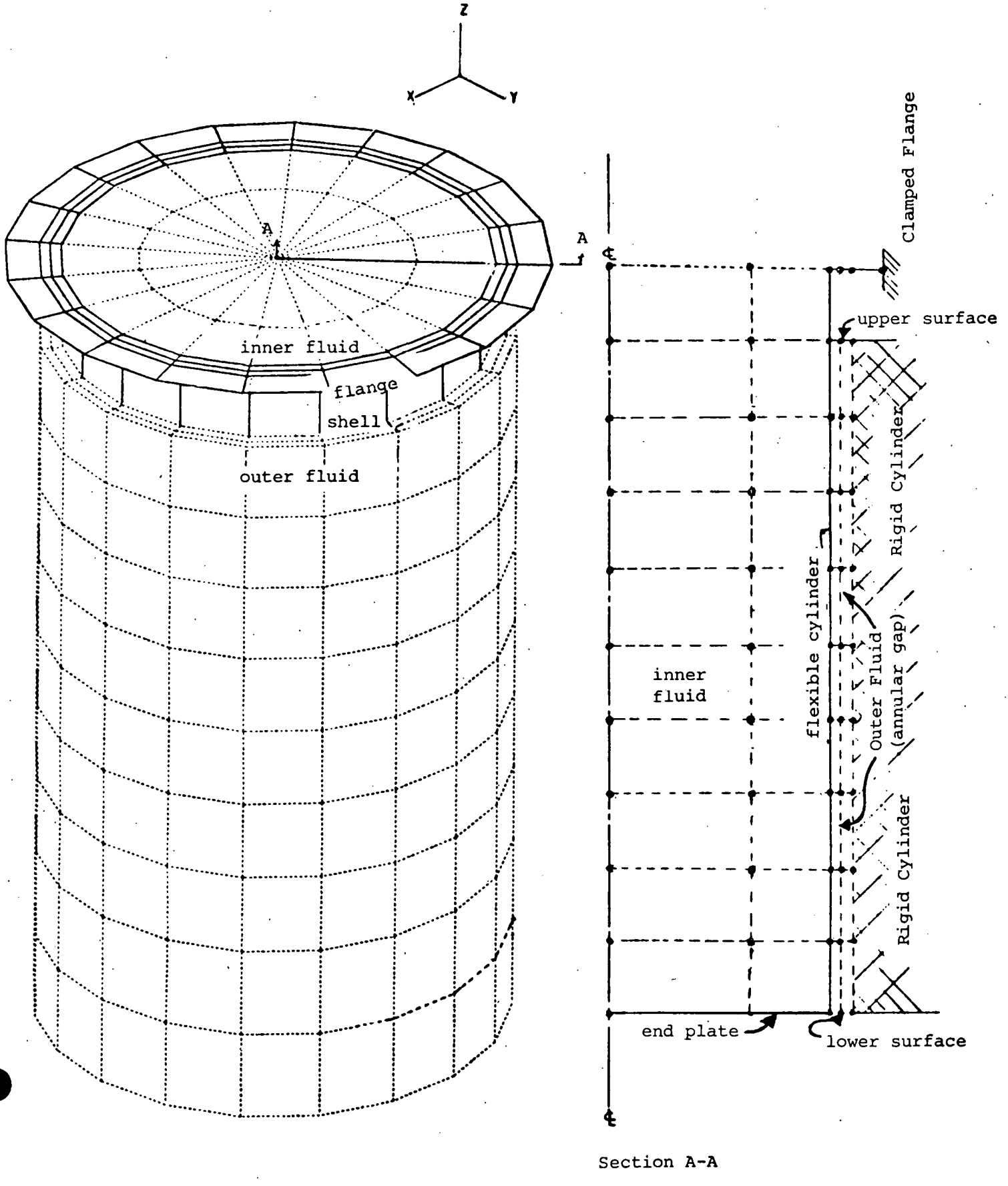
Z
X
Y
A
A
inner fluid
flange
shell
outer fluid
Clamped Flange
upper surface
Rigid Cylinder
flexible cylinder
Outer Fluid
(annular gap)
inner
fluid
Rigid Cylinder
end plate
lower surface

Section A-A

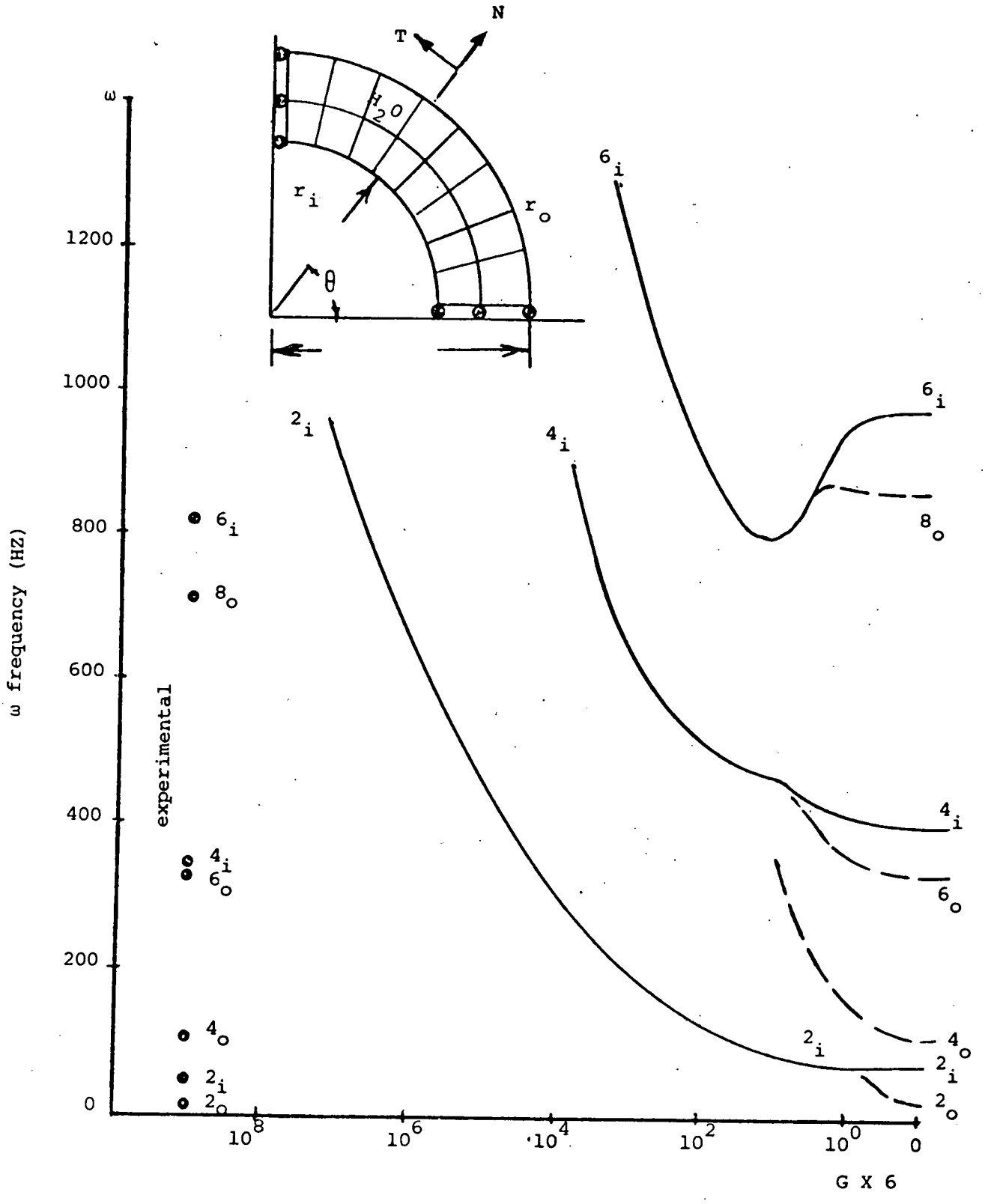

G (Shear Modulus - psi) X 6
(1 psi = 6.895 KPa)

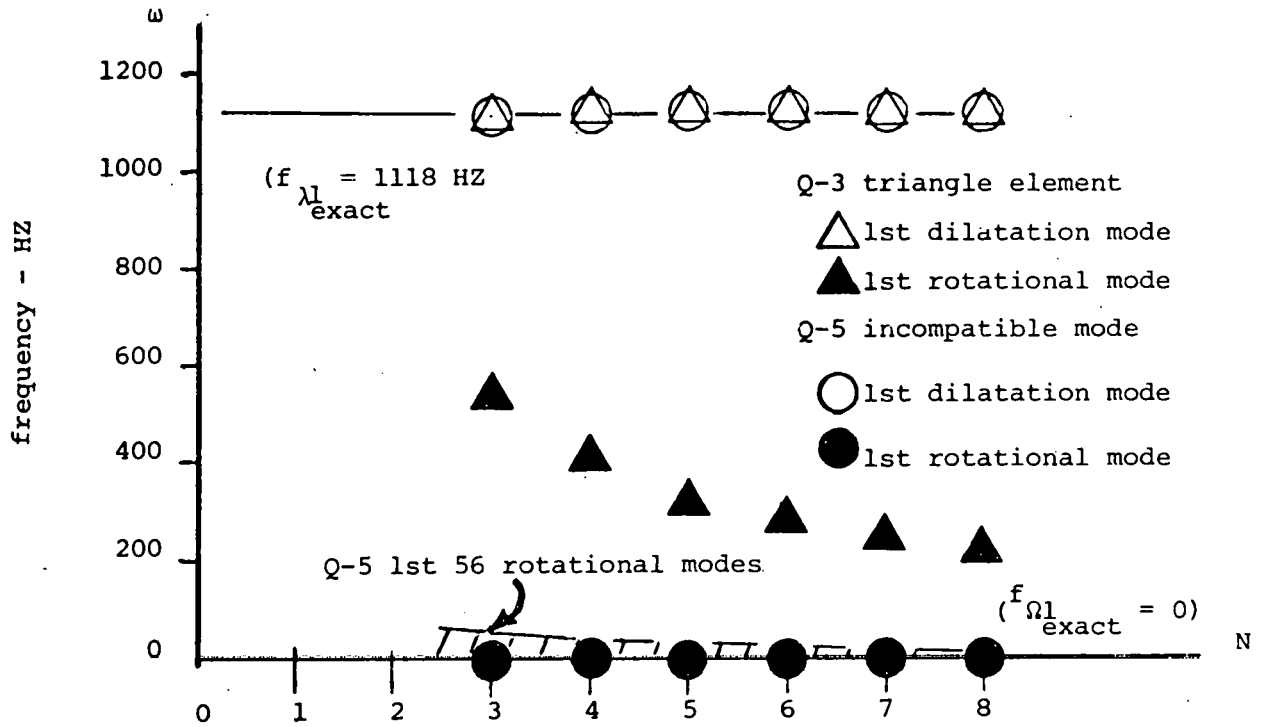

Element Refinement in A direction

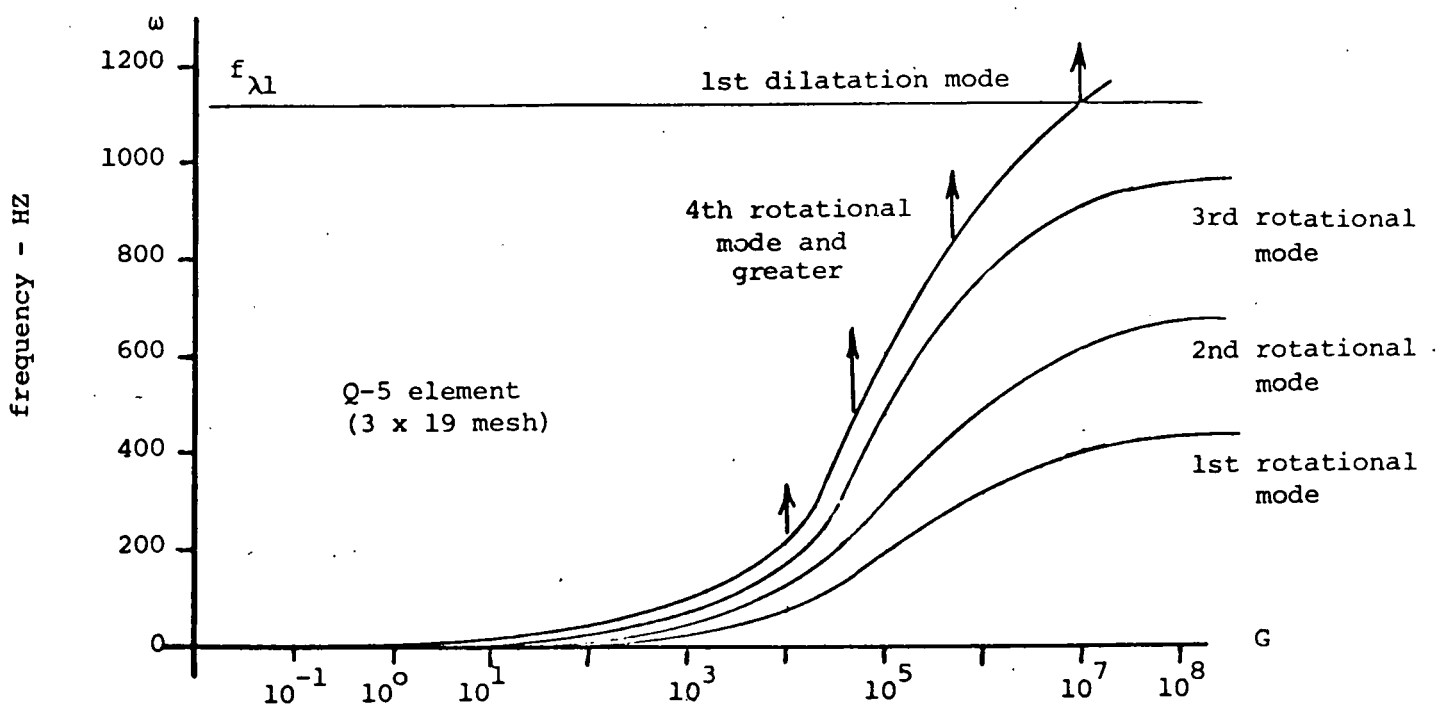

Shear Modulus G (psi)
(1 psi = 6.894 KPa)

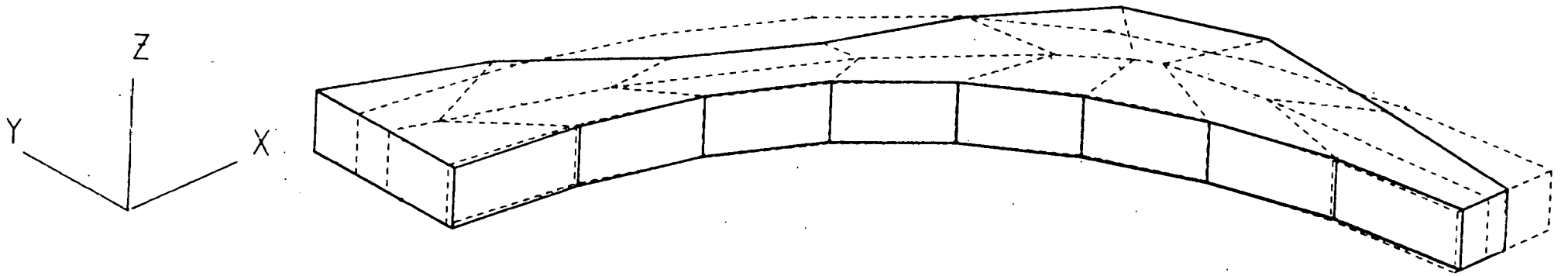
Z
Y
X

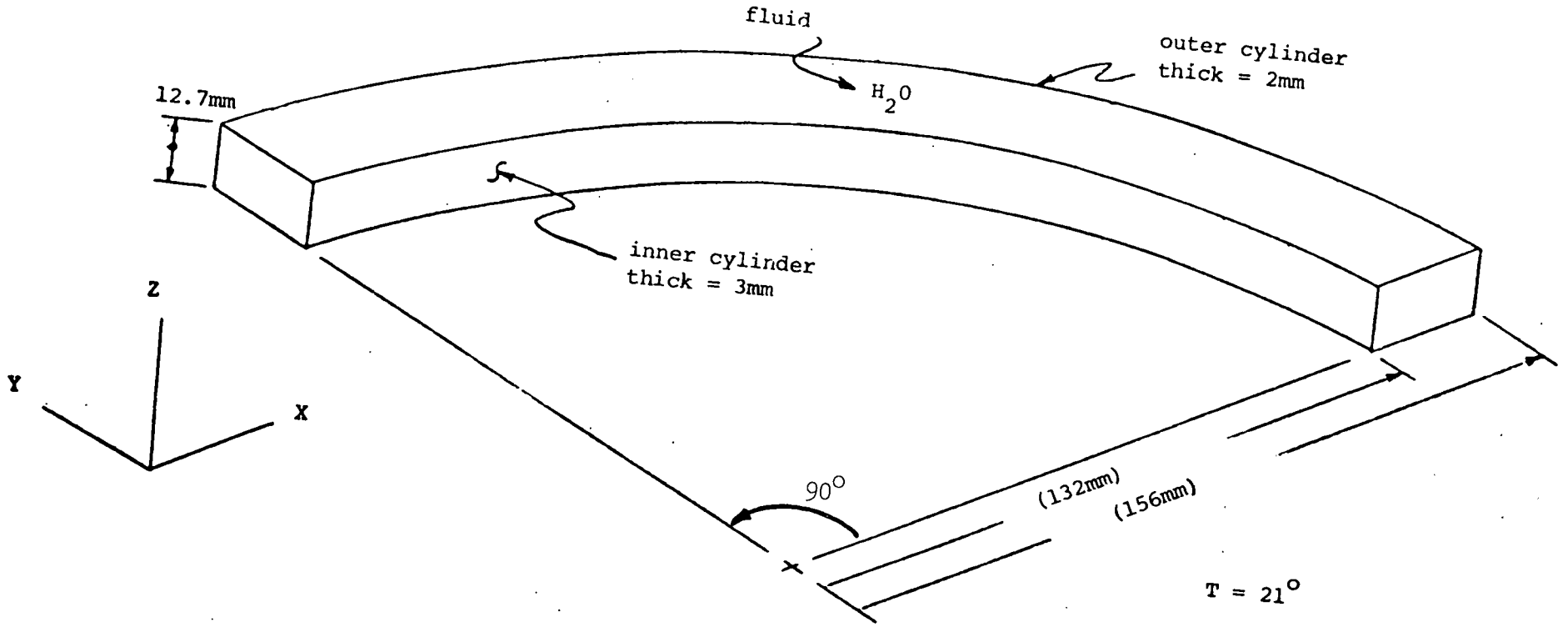
fluid
H_2O
outer cylinder
thick = 2mm
12.7mm
inner cylinder
thick = 3mm
Z
Y
X
90°
(132mm)
(156mm)
T = 21°